THE ASTROPHYSICAL JOURNAL, 437:827–840, 1994 December 20

INFRARED PHOTOMETRY AND SPECTROPHOTOMETRY OF NOVA HERCULIS 1991 (=V838 HERCULIS): OBSERVATIONS OF THE FORMATION OF DUST IN THE EJECTA OF A VERY FAST NOVA

THOMAS E. HARRISON[1] AND GUY S. STRINGFELLOW[2]
Mount Stromlo and Siding Springs Observatory, Australian National University,
Private Bag, Weston Creek P.O., Canberra, ACT 2611, Australia;
tharriso@nmsu.edu; guy@astro.psu.edu
Received 1992 October 8; accepted 1994 June 24

ABSTRACT

We present near-infrared photometry and spectrophotometry of Nova Herculis 1991 (N Her). Models of the near-infrared spectra of N Her reveal that shortly after visual maximum, the ejected gas was dense ($N_e \geq 10^{10}$ cm^{-3}), and cool ($T_e = 1000$ K). Models of the spectra also showed that as the first week following visual maximum progressed, the gas became hotter, and its density decreased. Within two days of visual maximum dust was condensing out of the ejecta. This limited dust formation began 5 days before the major dust shell formation event which occurred on, or near, 1991 March 31.8, 8 days after the initial outburst. This is the earliest time at which a dust shell has been observed to have been formed by a nova. The dust which formed in the ejecta of N Her was hotter ($T_d = 2000$ K) than previously observed for a nova. We find that the Clayton & Wickramasinghe (1976) model for the formation of carbon grains adequately explains the formation and evolution of the dust shell of N Her. We derive values of the outburst luminosity, the ejected gas and dust masses, and other parameters of the outburst of N Her, and compare these to published values.

Subject headings: dust, extinction — novae, cataclysmic variables — stars: individual (Nova Herculis 1991)

1. INTRODUCTION

Nova Herculis 1991 (=V838 Her, $\alpha_{1950} = 18^h44^m11^s.83$, $\delta_{1950} = +12°10'45''.0$; McNaught 1991) was a fairly bright, very fast nova that erupted toward the end of 1991 March (Sugano 1991; Alcock 1991). The presence of strong [Ne III] and [Ne V] emission lines in its optical spectrum (Dopita, Vassiliadis, & Ryder 1991) has led to it being classified as a member of the oxygen-neon-magnesium (ONeMg) subclass of novae (Starrfield, Sparks, & Truran 1986, and references therein), the eruptions of ONeMg novae eject material highly overabundant in oxygen, neon and magnesium. The primary in an ONeMg system is believed to be an ONeMg white dwarf, instead of the carbon-oxygen white dwarf believed to be common to most classical novae systems. Starrfield et al. (1986) have found that an explosion on a ONeMg white dwarf will eject more mass at higher velocities than the same eruption on a CO white dwarf of identical mass, yielding brighter visual maxima.

Past infrared studies of classical novae have been primarily limited to monitoring the broadband photometric temporal behavior of their light curves. Such studies have revealed that the ejected shells of many novae exhibit dust formation epochs (see Gehrz 1988 for a complete review). The observation of the formation of optically thick dust shells around novae (see Ney & Hatfield 1978), which reradiated the outburst luminosity of the nova in the infrared, confirmed the prediction of hydrodynamic models of novae outbursts (e.g., Sparks, Starrfield, & Truran 1976) that a post-outburst phase of constant bolometric luminosity existed.

The composition of the dust grains that have been observed to form in novae shells ranges from normal carbon dust (as in LW Ser: Gehrz et al. 1980b), to SiC dust (as in V1370 Aql; Gehrz et al. 1984), to emission tentatively attributed to polycyclic aromatic hydrocarbons (Greenhouse et al. 1990), to combinations of all of these (as in QV Vul; Gehrz et al. 1992). The physics and chemistry of dust formation in the circumnova environment is not well understood. The growth of grains may be hampered by the lack of nucleation centers and the low densities of condensate expected to be present in the expanding ejecta of novae (Gehrz 1988, and references therein). Clayton & Wickramasinghe (1976; hereafter CW) have proposed a model for the formation and growth of carbon dust in the ejecta of novae. As discussed by CW, carbon grains should condense once the temperature in the ejecta drops below $\sim$2000 K. At this temperature the partial pressure of carbon exceeds the vapor pressure of graphite. Prior to Nova Herculis 1991 (hereafter N Her), all novae dust shells had been observed to initiate grain growth at much lower temperatures near $\sim$1000 K (Gehrz 1988). We report herein observations of N Her which confirm the high-temperature dust formation scenario proposed by CW. The subsequent early evolution of the N Her dust shell is also well accounted for by this model. The late-time evolution of the dust shell, however, deviated from that predicted by the CW model—a period of grain destruction is suggested by our data. We propose that grain destruction, possibly by photodesorption, began shortly after dust shell maximum.

Infrared spectroscopic observations of novae have been mainly confined to circularly variable filter observations with resolutions of $\lambda/\Delta\lambda \sim 100$. This is due, in part, to the rapid decline in light that novae exhibit at infrared wavelengths, quickly fading below the limits of high-resolution infrared spectrometers. Fortunately, N Her was bright enough for us to obtain high-resolution spectrophotometry ($\lambda/\Delta\lambda \simeq 500$) during the first week following outburst. These spectra revealed that emission from dust grains was present two days after visual maximum, and several days before the main dust shell-

[1] Currently at the Department of Astronomy, New Mexico State University, Las Cruces, NM 88003.
[2] Currently at the Department of Astronomy and Astrophysics, Pennsylvania State University, 525 Davey Lab, University Park, PA 16802.

TABLE 1

INFRARED PHOTOMETRY OF NOVA HERCULIS 1991

U.T. Date	$(t - t_0)^a$	J	H	K	L	M
Mar 25.8.....	2.8	4.92 ± 0.03	4.57 ± 0.03	4.12 ± 0.03	3.45 ± 0.06	
Mar 26.8.....	3.8	5.68 ± 0.03	5.34 ± 0.03	4.77 ± 0.03	3.99 ± 0.06	
Mar 27.8.....	4.8	6.22 ± 0.03	6.09 ± 0.03	5.43 ± 0.03	4.55 ± 0.06	
Mar 30.8.....	7.8	6.93 ± 0.03	6.81 ± 0.03	6.04 ± 0.03	5.27 ± 0.06	4.73 ± 0.10
Mar 31.8.....	8.8	6.93 ± 0.03	6.04 ± 0.03	5.03 ± 0.03	4.03 ± 0.06	3.49 ± 0.10
Apr 28.7	36.7	9.95 ± 0.05	7.67 ± 0.05	5.74 ± 0.05	3.74 ± 0.10	
Apr 29.7	37.7	10.18 ± 0.05	7.81 ± 0.05	5.88 ± 0.05	3.88 ± 0.10	
Apr 30.7	38.7	10.29 ± 0.05	7.95 ± 0.05	5.95 ± 0.05	3.93 ± 0.10	
May 2.7.....	39.7	10.40 ± 0.04	8.02 ± 0.02	6.00 ± 0.02	4.13 ± 0.03	
May 3.6.....	41.6	10.78 ± 0.04	8.54 ± 0.04	6.31 ± 0.03	4.31 ± 0.03	
May 4.6.....	42.6	10.84 ± 0.04	8.39 ± 0.02	6.34 ± 0.03	4.29 ± 0.03	
May 5.6.....	43.6	11.01 ± 0.03	8.56 ± 0.03	6.48 ± 0.01	4.36 ± 0.04	
Jun 21.5	90.5	14.26 ± 0.08	13.13 ± 0.05	10.28 ± 0.03	7.07 ± 0.15	
Jun 22.6	91.6	13.99 ± 0.10	12.88 ± 0.10	10.28 ± 0.04	7.27 ± 0.10	
Aug 22.4.....	152.4	15.16 ± 0.14	15.25 ± 0.13	13.93 ± 0.04	10.67 ± 0.23	
Aug 26.4.....	156.4	15.18 ± 0.10	14.85 ± 0.11	14.00 ± 0.08	10.51 ± 0.26	
Sep 24.5	185.5	14.90 ± 0.16	14.84 ± 0.13	14.41 ± 0.20		
Sep 26.4	187.4	15.38 ± 0.23	14.55 ± 0.14	14.45 ± 0.12	10.49 ± 0.54	

[a] t_0 has been defined as 1991 March 23.0 (WGJL).

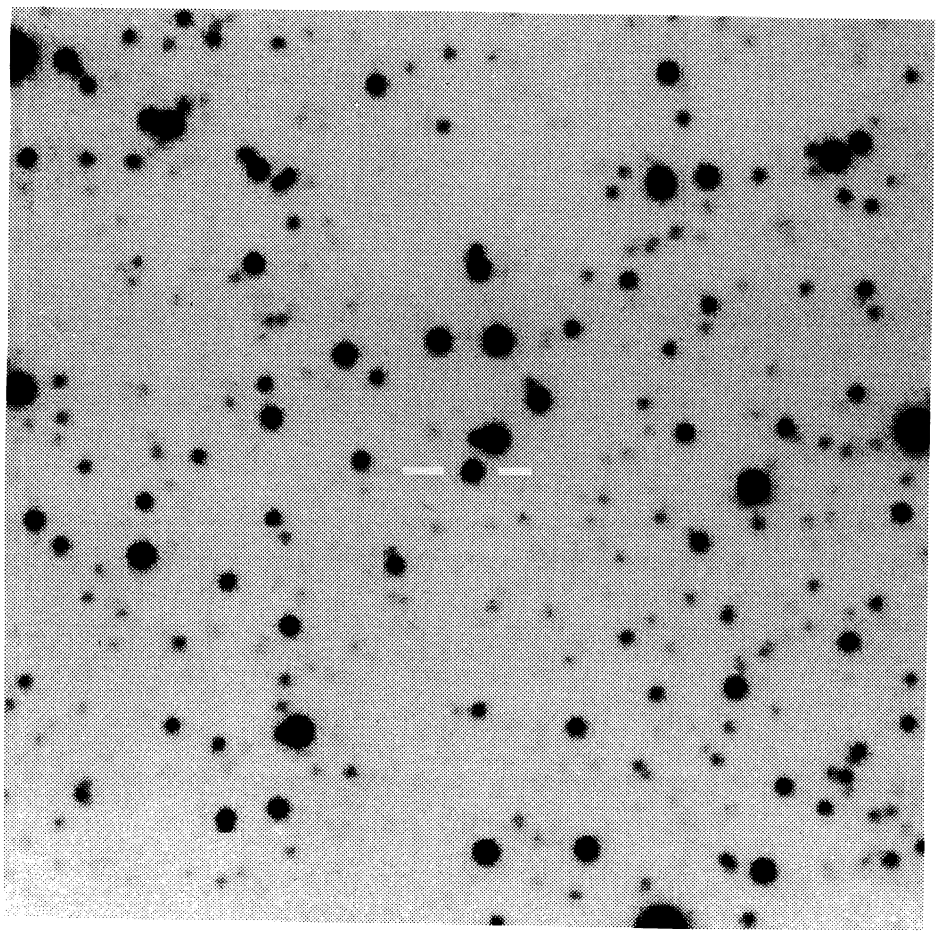

FIG. 1.—Gray scale CCD R band image of Nova Her and surrounding field obtained on 1991 July 12 with the 1 m telescope at Siding Springs Observatory. North is up, east is to the left. The image is 2′ × 2′.

formation event. The relative strengths of the hydrogen lines of the Brackett and Paschen series in the spectra of N Her enabled us to trace the density and temperature evolution of the expanding ejecta.

2. OBSERVATIONS

The photometric data presented in Table 1 were obtained using the Infrared Photometry System (IRPS; McGregor 1994) on the Siding Springs 2.3 meter telescope. The photometry was calibrated to the Mount Stromlo and Siding Spring Observatory system by observing standards listed in McGregor (1994). For the J, H, and K photometry, a 10″ aperture with a 20″ north-south throw was used. For some of the L' photometry, and for all of the M photometry, a 7″ aperture was used. As can be seen in Figure 1, a field star was located some 8″ to the NW of N Her. This faint star ($K \geq 12$) was excluded from our aperture in all the observations obtained after May.

The infrared spectra were obtained using the Cooled Infrared Grating Spectrometer (CIGS; Jones et al. 1982) on the 2.3 m telescope. The G dwarf spectral standards α Cen A (BS 5459), BS 5868, and BS 6094 were observed in order to remove terrestrial absorption features from the spectra, and to flux calibrate the data. The spectral resolution was $\lambda/\Delta\lambda \simeq 500$ for the 25.8, 26.8, 27.8, and 30.8 March observations, and $\lambda/\Delta\lambda \simeq 200$ for the 31.8 March observation. All of the spectra have been flux calibrated using the FIGFLUX routine in the STARLINK software package FIGARO (Cohen 1988).

3. THE INFRARED DEVELOPMENT OF NOVA HERCULIS

N Her was first sighted by Sugano (1991) on 1991 March 24.8 UT (JD 2448340.3) at $m_V = 5.4$. Because the initial rise to maxima in novae can be very brief, frequently taking less than 1 day, the maxima for very fast novae like N Her are often missed. For example, N Her declined by two magnitudes within the first 1.4 days following discovery (Fig. 2). The last upper limit observation for N Her, March 23.77 (Yamamoto 1991), falls about 24 hours before the discovery observation. This prediscovery limit suggests that the discovery observation of March 24.8 was close to the time of actual visual maximum. The actual outburst would have occurred before visual maximum, and the assignment of the data of the initiation of the outburst to March 23.0 ± 1 by Woodward et al. (1992, hereafter WGJL) is reasonable, and we will reference our observations to this data (hereafter t_0) for the remainder of this paper.

3.1. *Infrared Photometry*

Our first infrared observations were obtained on March 25.8, 24 hours after discovery. The infrared spectral energy distribution for this date, and its evolution over the next 6 months, is presented in Figures 3*a*–3*c*. While the infrared photometry for March 25.8 is reasonably well fitted by a $T \sim$ 3000 K blackbody, the inclusion of the V-magnitude estimate for this date ($V = 7.1$, Sonneborn, Shore, & Starrfield 1991), rules out such an energy distribution. No combination of reddening and blackbody temperature results in a reasonable

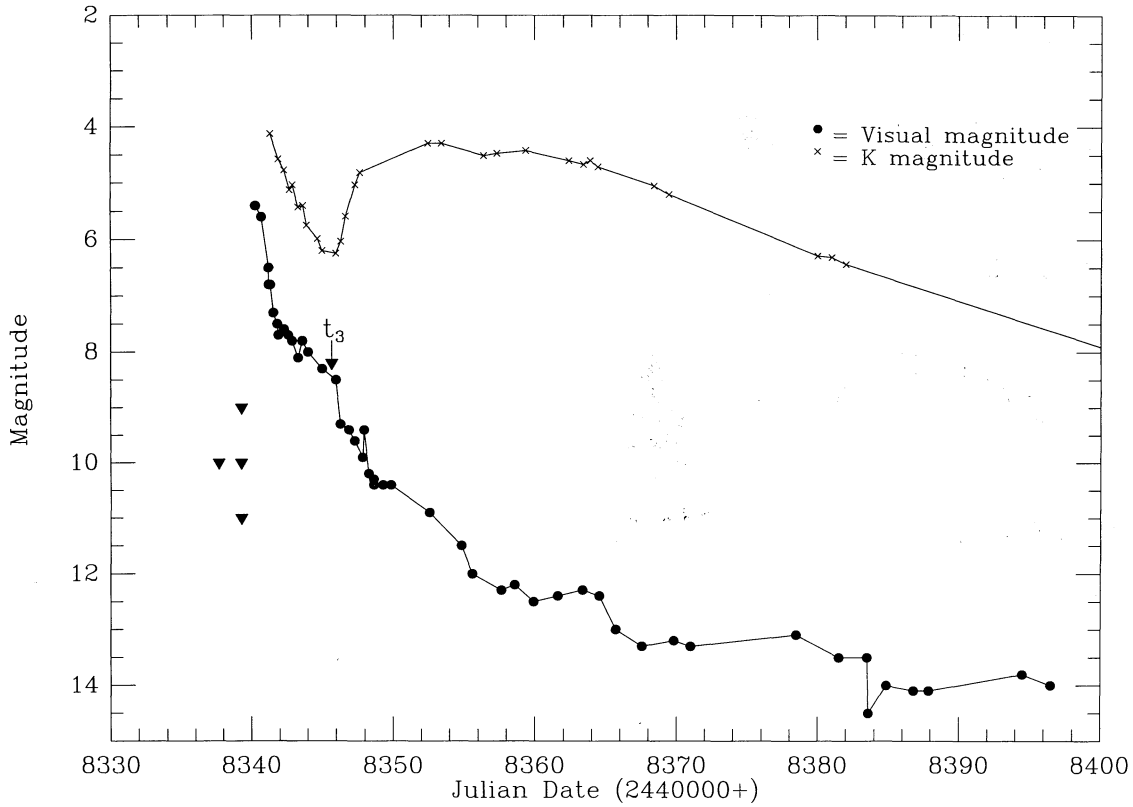

FIG. 2.—Visual (*solid circles*) and K-band (*crosses*) lightcurves of Nova Herculis 1991 taken from the literature and numerous IAU Circulars. Triangles represent upper limits to the brightness of N Her. The sudden rise in the K-band lightcurve, which signals the formation of the dust shell, is accompanied by a rapid 1 magnitude drop in the visual light. The time for the visual light to decline by three magnitudes from maximum, t_3, is indicated.

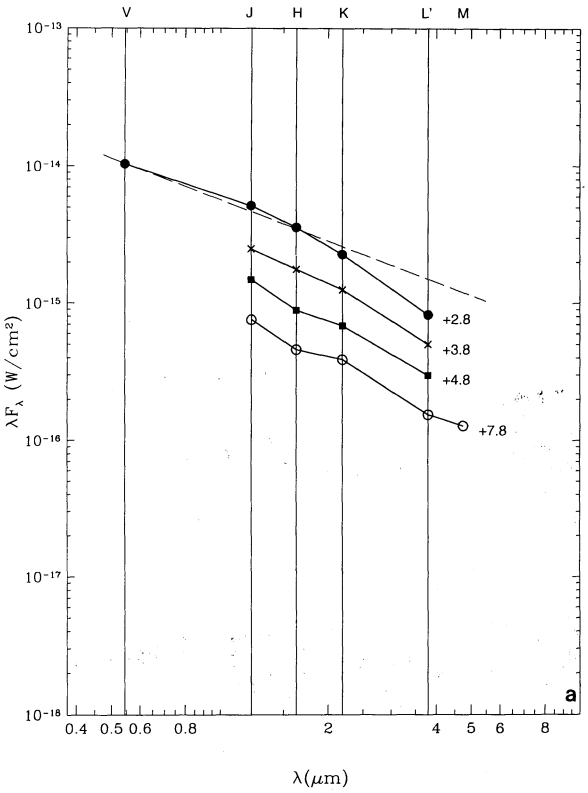

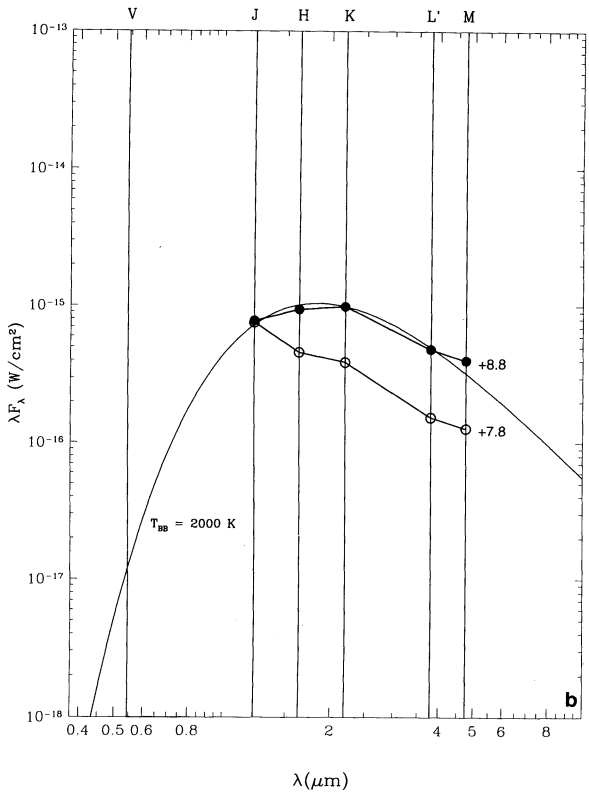

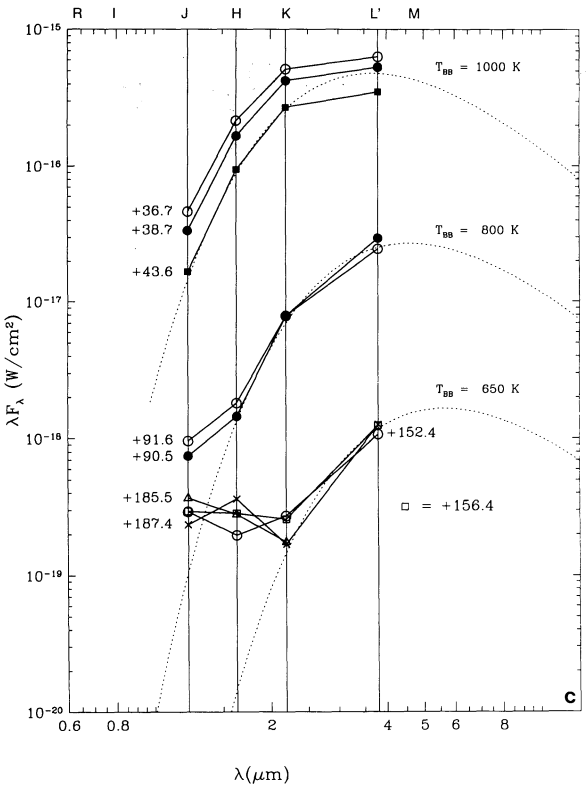

FIG. 3.—(*a*) Spectral energy distributions [log (λF_λ) vs. log (λ)] for Nova Herculis. The photometry from March 25.8 (*solid circles*), to March 30.8 (*open circles*). The photometry has been de-reddened using a visual extinction of 1.4 mag. The dereddened photometry for March 25.8 is inconsistent with a blackbody energy distribution. The *V*, *J*, and *H* photometry is reasonably well fit by a free-free energy distribution (*dashed line*) which becomes optically thick at $\lambda > 2.0$ μm. The time in days since t_0 of the plotted photometry is indicated. (*b*) The major dust shell-formation event occurs within 24 hours between March 30.8 (*open circles*) and March 31.8 (*filled circles*). The photometry for March 31.8 has been fitted by a blackbody with a temperature of 2000 K. The time in days since t_0 of the plotted photometry is indicated. (*c*) Late-time decline of the infrared spectral energy distribution. From mid-April to mid-June (for clarity, not all of the data obtained in this interval have been plotted), the photometry can be modeled by a dust shell with a color temperature of $T_{BB} \approx 1000$ K. The dust shell cooled as it expanded over the subsequent 6 months. Eventually, emission from other processes in the shell dominates the emission from the dust shell at the shorter wavelengths. The time in days since t_0 of the plotted photometry is indicated.

fit to the available photometry. It appears that within 1 day of visual maximum the ejecta were already optically thin well into the near-infrared. This conclusion is confirmed by the existence of H I emission lines throughout the near-infrared spectrum of N Her for this date, obtained within minutes of the near-infrared photometry. The following day, March 26.8, the infrared energy distribution had evolved to one that resembled the energy distribution of free-free emission. Over the next 4 days the energy distribution maintained the same overall shape, but with a rapid flux decline.

In the 24 hours between March 30.8 and 31.8 the infrared energy distribution of N Her changed dramatically (Fig. 3*b*). In this interval the energy distribution changed from a free-free–like energy distribution to that of a 2000 K blackbody. The dramatic change can be explained as the onset of dust formation in the ejected shell of N Her. As noted by WGJL, a drop of ~ 1 mag in the visual light curve appears to temporally correspond with the onset of the formation of the dust "shell" (Fig. 2). *The formation time of 8 days after outburst makes this the earliest epoch at which dust has been observed to have formed for any nova.*

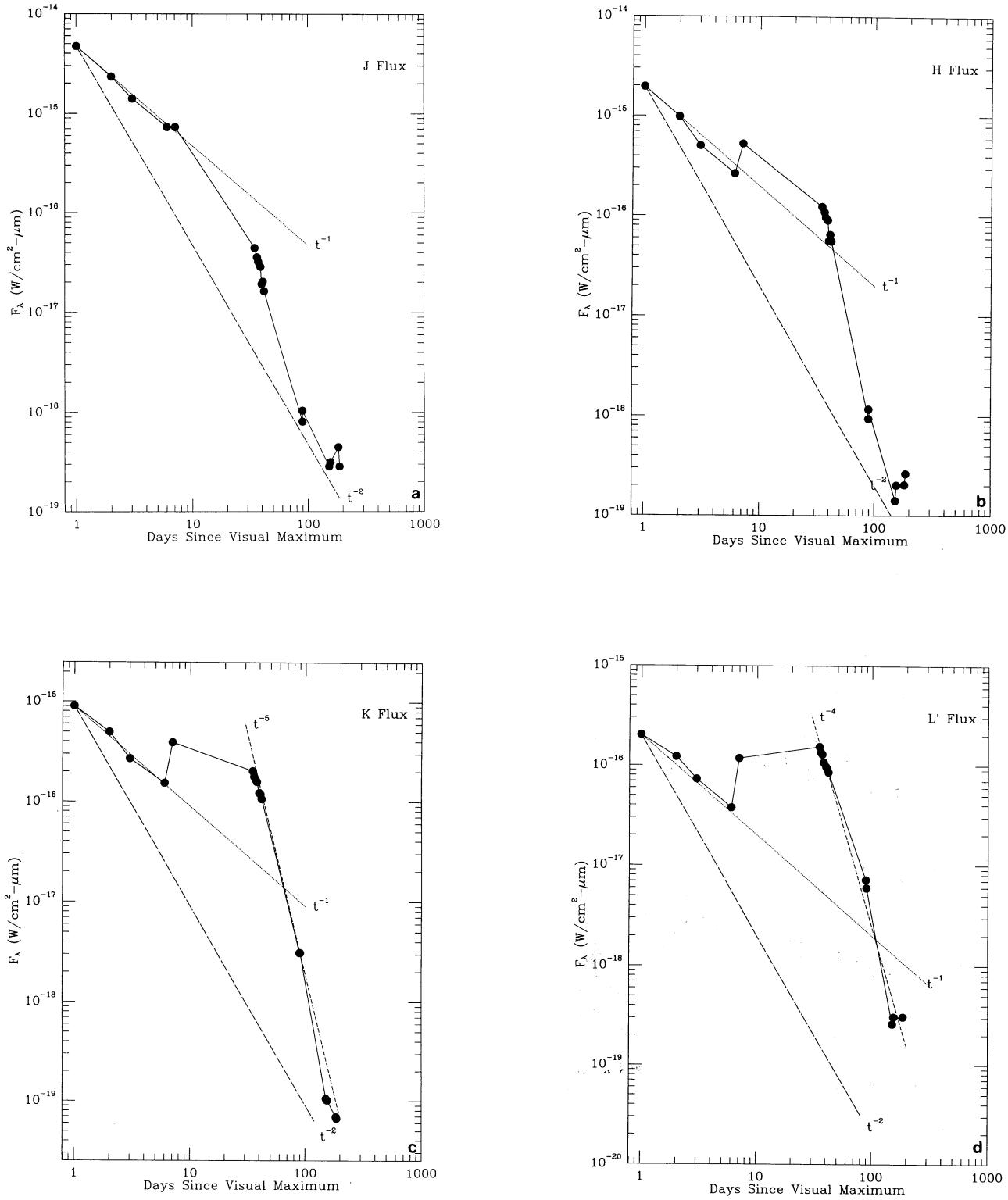

FIG. 4.—(*a*) Temporal evolution of the *J*-band flux. The early decline is well represented by a $F_\lambda \propto t^{-1}$ dependence (*dotted line*). After dust shell formation, the flux declines at a more rapid rate. Eventually, the rate of decline matches up to a t^{-2} rate of decline (*dashed line*). Boyarchuk & Gershberg (1977) have shown that such a decline is representative of a gas shell ejected in a polar-cone-equatorial disk configuration. (*b*) Temporal evolution of the *H*-band flux. Like the *J*-band, the early decline in the flux at *H* is well represented by a t^{-1} relationship (*dotted line*). After the formation of the dust shell, there is period of increased flux in the *H*-band, after which the flux began a steep decline. The flux eventually approaches a t^{-2} relationship (*dashed line*) at late times. (*c*) Evolution of the flux at *K* is nearly identical to that at *H*, with an early decline $\propto t^{-1}$ (*dotted line*), a rise at the time of dust formation, a steep decline ($\propto t^{-5}$, *short-dashed line*), returning to an overall decline rate of t^{-2} at late times (*long-dashed line*). (*d*) Flux evolution in the *L*′ band. The early decline rate $\propto t^{-1}$ is again seen (*dotted line*). The flux at *L* evolves similarly to that at *K*, however, it never reaches the t^{-2} relation (*long-dashed line*) seen in the other bands due to emission from dust continuing to dominate the emission from the gaseous shell.

The evolution of the infrared energy distribution over the next six months is shown in Figure 3*c*. The energy distribution continued to be well modeled by a blackbody energy distribution during April and May. After May, as N Her continued to fade, sources of emission other than the dust shell became evident. For example, in the June 21.5 and 22.6 observations, the J flux is significantly elevated above the blackbody fitted to the H, K, and L' fluxes. As the nova continued to fade, the fluxes in both the J and H bands deviated from the warm blackbody fitted to the K and L' photometry. The behavior of the near-infrared fluxes in August and September is interesting: the H-band flux increased during this period, while the J-band flux remained nearly constant.

In the early stages of decline, the fluxes in the J, H, K, and L' bands (Figs. 4*a*–4*d*) declined as $F_\lambda \propto t^{-1}$. Ennis et al. (1977) have shown that the infrared flux from an ionized, spherical, optically thin expanding gas shell should decline as $F_\lambda \propto t^{-2}$ in the early stages (before the shell thickness has had time to expand), and later as $F_\lambda \propto t^{-3}$ in the "free expansion" phase. That the flux from N Her did *not* behave this way indicates that modeling the ejecta as a thin spherical shell is inappropriate. Novae ejecta are notoriously clumpy (see Gallagher & Anderson 1976, and references therein), and this clumpiness would certainly affect the flux decline rate. It is interesting that at very late times the J-, H-, and K-band fluxes are tending towards an *overall* decline rate proportional to t^{-2}. Boyarchuk & Gershberg (1977) have shown that a flux dependence $F_\lambda \propto t^{-2}$ is characteristic of gas ejected in a polar cone-equatorial disk configuration.

An alternative explanation of the t^{-1} rate of flux decline can be obtained by assuming that emission from something besides the gas was present, such as dust. We show below that limited dust grain formation was occurring in the ejecta of N Her within two days of visual maximum. Emission from changing quantities of dust could mask the actual flux decline rate of the emission from the gaseous component of the ejecta, strongly affecting the observed decline rate.

3.2. *Infrared Spectroscopic Observations*

Infrared spectroscopic observations were obtained immediately following the photometric observations during the first week following maximum. These spectra are displayed in Figures 5*a*–5*e*. The spectrum for March 25.8 (Fig. 5*a*) has a number of interesting features. The strongest lines in the spectrum for this date were the hydrogen lines Brγ, Br 10–13, Paβ, and Paγ. Weak He I emission lines at 1.0830 μm and at 2.058 μm were also present. A strong line at 1.13 μm could be assigned to either the O I triplet (1.1287 μm), or S I (1.1309 μm). The profiles of some of the hydrogen and helium lines (notably He I 2.058 μm) in the spectra of N Her for this date, and the remainder of the week, appeared to have had multiple peaks, similar to what was observed in optical spectra (see Feast 1991). We obtain a FWHM velocity of 3500 km s^{-1} from a Gaussian fit to the profiles of the strongest infrared H I lines.

Determination of the continuum level for the March 25.8 spectrum is difficult. If we define the continuum level by connecting the minima in the spectrum in the wavelength range 1.05 to 1.80 μm to the first part of the K band, a flat continuum level results. If this was the true continuum level, then significant excess emission was occurring in the J band longward of $\lambda = 1.17$ μm. A number of distinct spectral lines, besides those mentioned above, were located at 1.172, 1.200, 1.50, and 1.770 μm. Evans et al. (1990) have suggested a series of N I and C I lines to explain a broad feature seen in their spectra of PW Vul at $\lambda \simeq 1.75$ μm. In those spectra, however, a strong line of C I also appears a 1.69 μm. No such line is evident in the H-band spectrum of N Her, leaving nitrogen to explain the feature at 1.770 μm. One atomic species presumably abundant in the ejecta of N Her is neon. Of the various ionization states of neon, only [Ne I] has emission lines in the J, H, and K bands. The near-infrared spectrum of [Ne I] contains numerous lines arranged in bands. Nebular modeling of [Ne I] emission will be necessary to determine whether it can be used to explain the J-band excess and other unidentified features present in the spectrum of N Her for March 25.8.

One molecule which simultaneously explains both the J excess at $\lambda \geq 1.17$ μm, as well as the individual spectral features at 1.172, 1.200, 1.50, and 1.770 μm is C_2, which has bandheads located at 1.175, 1.209, 1.45, and 1.775 μm (Johnson et al. 1983). To our knowledge, infrared C_2 emission has never been observed from a stellar source, being confined to solar (Brault et al. 1982) and stellar absorption features (especially in carbon stars, see Goebel et al. 1980). Infrared C_2 emission has been observed in the spectra of comets (see Johnson et al. 1983). As is the case in red giants, the presence of C_2 features in the spectrum of N Her would imply that the ejecta of N Her were underabundant in oxygen, or else the carbon would have quickly combined with oxygen to form CO. It is interesting to note that analysis of optical spectra by Matheson et al. (1993) seem to indicate that oxygen was relatively *underabundant* in the ejecta of N Her. Optical spectra obtained during the first week following visual maximum should be examined for C_2 emission features (the Swan bands).

During the next 24 hours, the excitation level of the ejecta had markedly increased (March 27.8, Fig. 5*b*). This is evident by the strengthening of the He I lines at 1.0830 μm (blended with H I Paγ) and 2.058 μm. The excess in the J band has weakened, revealing apparent emission lines at 1.247, 1.311, and 1.338 μm. The emission lines formerly present at 1.134, 1.172, and 1.200 μm have also weakened. The broad feature at 1.77 μm, tentatively assigned to N I above, is still present. In PW Vul, Evans et al. (1990) identified further N I features at 1.233, 1.238, 1.246, 1.247 μm. Such a group of lines could explain part of the J-band excess noted above for March 25.8, as well as the multipeaked feature located near 1.247 μm in the spectrum for this date. The emergence of the double-peaked He I lines is the greatest change in the 24 hours between spectra, with He I 1.0830 μm now dominating H I Paγ. The continuum level for March 26.8 spectrum is much simpler to derive than for the previous day, and has a gentle slope with increasing flux toward the red end of the spectrum.

Little overall change was evident in the spectrum of N Her between March 26.8 and 27.8 (Fig. 5*c*), the exceptions being the increasing relative strength of the He I lines, and the abrupt change in the H-band spectrum at $\lambda \geq 1.75$ μm. The strengthening of the He I lines continues to indicate an increasing excitation level of the ejecta. The change in the spectrum longward of H I Br 10 is dramatic. The feature formerly present at $\lambda = 1.77$ μm in the two earlier spectra has completely disappeared, being replaced by a complex feature at a slightly longer wavelength ($\lambda \sim 1.78$ μm). The fluxes of the last portion of this feature are highly uncertain due to a difficult flux calibration that is strongly affected by terrestrial absorption. The weak feature at 1.5 μm is still present. The continuum of this spectrum is significantly redder than that of the previous 2 days; we

1994ApJ...437..827H

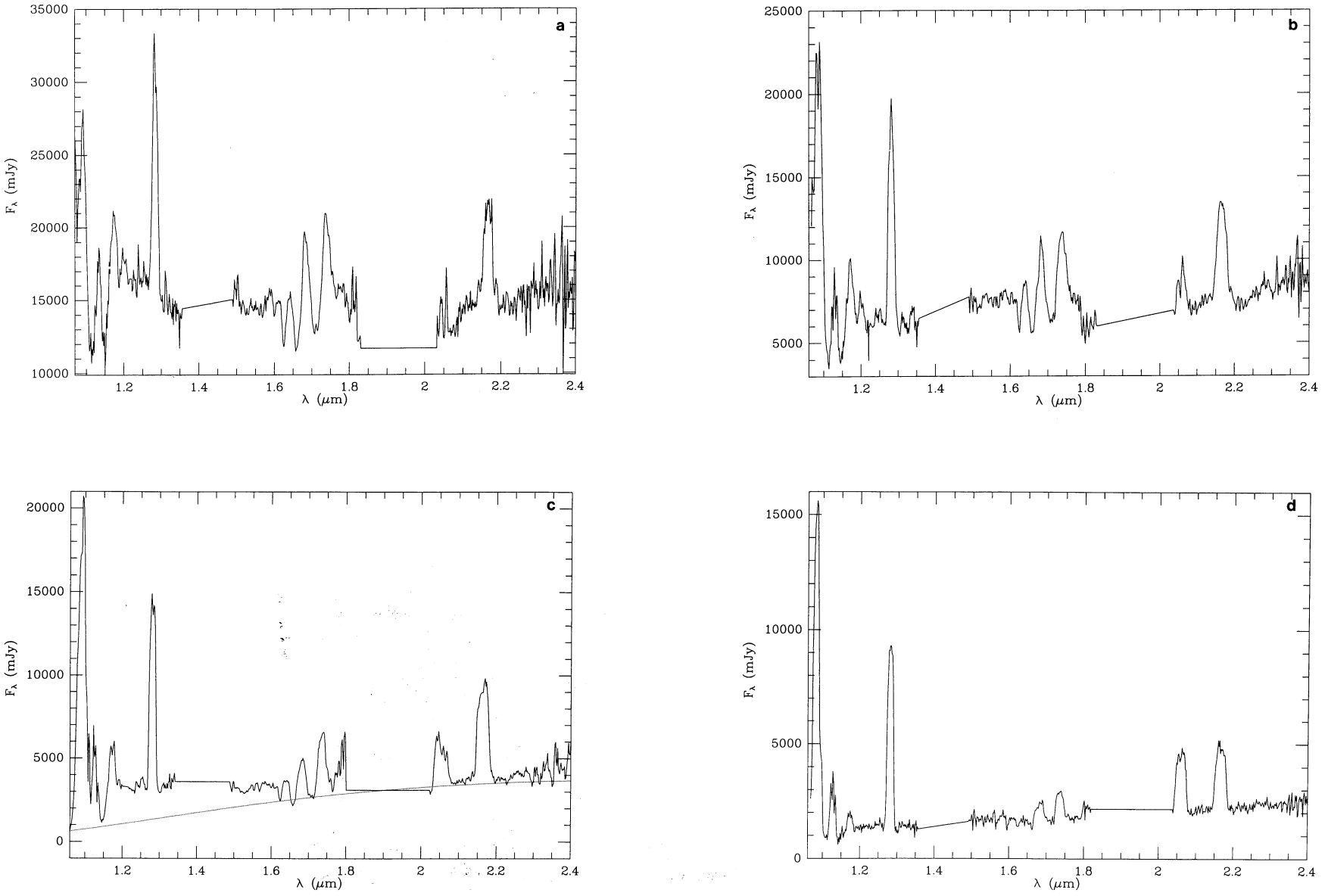

FIG. 5.—(*a*) Infrared spectrum of N Her for March 25.8. The existence of H I emission lines throughout the near-infrared spectrum for this date shows that the ejecta had already become optically thin within 1 day of visual maximum. The weakness of the H I Brγ (2.16 μm) line with respect to the H I lines in the *J* and *H* bands indicates that the ejecta may have been optically thick at $\lambda > 2.0$ μm. The strongest line in the spectrum for this date is H I Paβ (1.28 μm). A fit to the lowest points in the continuum for this date results in a considerable *J*-band excess at $\lambda > 1.17$ μm. (*b*) Infrared spectrum of N Her for March 26.8. The most dramatic change between this spectrum and that of the previous day is the strengthening of the He I lines (at 1.083 and 2.06 μm). (*c*) Spectrum for March 27.8. The continued strengthening of the He I lines is evident. A feature at $\lambda \simeq 1.77$ μm has suddenly appeared. A reddened (by $A_V = 1.4$ mag) 2000 K graybody source (*dotted line*) supplies nearly the entire *K*-band continuum, while providing a reasonable fit to the lowest points of the continuum in both *J* and *H* bands. (*d*) Spectrum for March 30.8. The He I line at 2.06 μm now rivals H I Brγ in strength, indicating the rapid rise in the excitation level of the ejecta. (*e*) Low-resolution spectrum of N Her for March 31.8. The continuum has become much redder after the formation of the dust shell. The continuum is well modeled by a 2000 K blackbody source (*dotted line*), in agreement with the dust shell temperature derived from the photometry for this date.

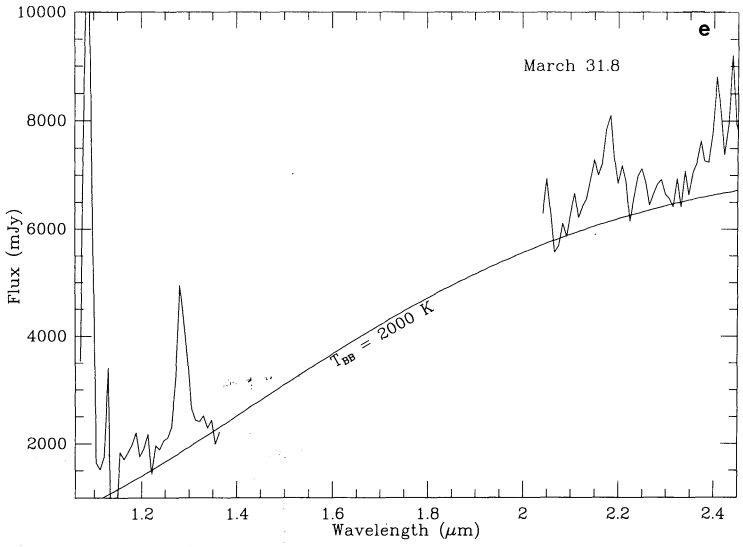

FIG. 5—*Continued*

argue below that the origin of this red continuum is emission from a small quantity of dust in the ejecta.

The spectrum for March 30.8 (Fig. 5*d*) is dominated by the He I 1.0830 μm line, the He I line at 2.058 μm now rivals H I Brγ in strength, and the He I line at 1.700 μm now distorts the profile of the H I Br 10 line. The excess in the *J* band has nearly disappeared. The only *lines* in the spectrum not attributable to hydrogen or helium are those at 1.13 and 1.17 μm, whose continued strength is interesting. These two lines have been visible since the first spectrum, when the ionization state of the ejecta was very low, and have remained strong as the excitation level has increased. This suggests to us that the species responsible for this emission are highly abundant, and have an excitation level not too different from that of hydrogen. While both neutral oxygen and sulfur fit this description, and can explain the 1.13 μm line, we have been unable to associate the 1.17 μm line with these, or any other atomic species.

As seen in the photometry, the transition from a nebular distribution on March 30.8, to a graybody energy distribution on March 31.8, is apparent in the spectra for those two dates (Figs. 5*d* and 5*e*, respectively). The only emission lines present in the low resolution spectrum obtained on March 31.8 are H I Brγ and Paβ, and He I (1.0830 and 2.06 μm). The steep red continuum is well modeled by a 2000 K blackbody source.

4. CHARACTERIZING THE OUTBURST OF N HERCULIS, AND EVOLUTION OF THE CIRCUMSTELLAR EJECTA

The photometry discussed above shows that N Her developed a dust shell at an earlier epoch than any other known nova. This fact was further supported by the analysis of the contemporaneous near-infrared spectroscopy. We now attempt to quantify many of the parameters of the outburst of N Her, and trace the evolution of both the gaseous and dust components of the ejecta.

4.1. *Outburst Luminosity, Distance, and Reddening*

As can be seen from the visual light curve shown in Figure 2, the rate of visual decline was extremely fast. The time to decline by 3 magnitudes from maximum (t_3) was only 5.3 days. This rapid decline rate makes N Her one of the fastest of all novae, rivaling MU Serpentis as the second fastest of known novae, with decline rates only slightly slower than V1500 Cyg (t_3 = 3.6 days, Vogt 1990). The t_3 which we derive for N Her is slightly longer than that found by WGJL, but significantly longer than that derived by Lynch et al. (1992). This latter difference arises because we have chosen not to use the visual magnitude estimate of $m_v = 5$ (Alcock 1991) in our light curve because of the low precision of this estimate, and because a nearly simultaneous visual estimate by Buczynski (1991) places N Her much fainter at $m_V = 5.6$. Using the relationship between rate of decline and absolute visual magnitude at maximum for classical novae [$M_V = -11.5 + 2.5 \log (t_3)$; McLaughlin 1960], we derive an absolute visual magnitude at maximum of $M_V = -9.7$.

Because the bolometric corrections of novae at maximum are small (van den Bergh & Younger 1987), the absolute visual magnitude at maximum is approximately equal to the bolometric magnitude at maximum. With $M_V = -9.7$, the outburst luminosity of N Her at maximum was $5.9 \times 10^5\ L_\odot$. This is a factor of ~ 13 above the Eddington luminosity of 1.4 $M_\odot$ white dwarf. WGJL found such a large luminosity difficult to accept, however, such super-Eddington luminosities are not unknown in other novae. For example, V1500 Cyg achieved a luminosity of nearly $10^6\ L_\odot$ near maximum (Lance, McCall, & Uomoto 1988), while the recurrent nova T CrB reached an outburst luminosity of $2 \times 10^5\ L_\odot$ at maximum (Harrison, Johnson, & Spyromilio 1993). Starrfield et al. (1986) have shown that the outbursts resulting from a thermonuclear runaway on an ONeMg white dwarf can exceed the Eddington luminosity at bolometric maximum. We present analysis below that confirms the high outburst luminosity of N Her.

Without observations of N Her when its gaseous shell was in an optically thick, pseudo-photospheric phase, an accurate estimate of the visual extinction is impossible to derive from the infrared photometry alone. If, however, the free-free fit (see Fig. 3*a*) of the *J*, *H*, and *K* photometry is extrapolated to visual wavelengths, with the assumption that the visual light is likewise dominated by free-free emission at this time, then we find a visual extinction of $A_V = 1.4$ mag to N Her. This is somewhat greater than the $A_V = 1$ mag that WGJL derive from post-maximum optical photometry of N Her, but closer to the value of $A_V = 1.7$ mag found by Lynch et al. (1992) from an analysis

of the interstellar Na D lines. van den Bergh & Younger (1987) have shown that the unreddened $B-V$ colors of novae at t_2, the time taken to fall 2 magnitudes from maximum, are $(B-V)_0|_{t_2} = -0.02 \pm 0.04$. The date for t_2 was March 26.2; $t_2 = 1.4$ days. UBV photometry by Della Valle & Turrato (1991) on March 26.4 yielded $B-V = 0.51 \pm 0.1$, leading to a visual extinction estimate of $A_V = 1.6 \pm 0.3$ mag. Another estimate of the reddening comes from the method derived by Miroshnichenko (1988) who found that during the "stabilization state" (a plateau in the change of $U-B$ and $B-V$ as the novae declines), the average $B-V$ colors of novae are $\langle B-V\rangle_{ss} = -0.11$, or $A_V = 3.1\ [(B-V)_{obs} + 0.11]$. From optical photometry by Izumo & Oshima (1991), and Harrison & Stringfellow (1994), it appears that N Her underwent a short stabilization state during early April. During this period $\langle B-V\rangle \simeq 0.35$, yielding a visual extinction of $A_V = 1.4$ mag.

These estimates for the visual extinction are consistent with that for the open cluster NGC 6709 which is on a similar line-of-sight as N Her. Sowell (1987) lists NGC 6709 as having an extinction of $A_V = 0.9$ mag, and a distance of 910 pc. We will assume for the remainder of this paper that the visual extinction to N Her is $A_V = 1.4$ mag. Using this extinction, and the apparent and absolute visual magnitudes at maximum, the distance to N Her is $D = 5.5$ kpc. This value is higher than that determined by WGJL, Starrfield et al. (1992), or Lynch et al. (1992), but only about one-half of that found by either Chandrasekhar et al. (1992), or Lloyd et al. (1992). We have tabulated the results of the published values for the distance and other derived parameters of the outburst of N Her in Table 2.

4.2. *Modeling the Infrared Spectra: Determination of the Temperature and Density Evolution of the Ejecta*

To enable us to use the H I lines in the infrared spectra to determine the temperatures and densities present in the ejecta, we have devised a spectrum modeling program to add both reddened free-free and blackbody continua to properly reddened, normalized, and velocity-broadened H I lines. Hummer & Storey (1987, hereafter HS) have tabulated the strengths of the H I lines for the wide range of temperatures and densities for which the case B assumption (Lyman series optically thick) is valid. The interpolation methods described by HS, allowing the calculation of the line strengths at temperatures and densities intermediate to those tabulated, have also been included in the modeling program. Where appropriate, we have included the opacities of the H I Paschen lines. Given the interstellar extinction, the physical conditions of the ejecta can be determined if the assumption of case B conditions is valid.

We begin by modeling the March 25.8 spectrum. The spectrum for this date is somewhat peculiar in that the Brγ line is substantially weaker than expected given the strengths of the other lines in the Brackett series. The profile of this line also exhibits considerable structure. The photometry for this date suggests that the ejecta may have still been partially optically thick longward of 2 μm (note the depression in the K and L' fluxes in Fig. 3*a* for March 25.8 relative to the following days). Thus it is uncertain whether the ejecta completely satisfy case B conditions at the time of this first spectrum. The H I Paschen lines (Paα and γ), the Brackett series (Br 10 to 14) and the Brackett continuum, however, appeared to have been optically thin at this time. After investigating models covering the complete range of temperatures and densities available in HS, we find a best fit to the March 25.8 spectrum results with an electron density of $n_e = 10^{10}$ cm^{-3}, and an electron temperature of $T_e = 1000$ K: the highest density, lowest electron temperature combination tabulated by HS. From trends in the modeling process, it would appear that a higher density would produce a spectrum that would fit the observed one more closely. The model fit to the spectrum for March 25.8 was not as good as those achieved on following days.

Ennis et al. (1977), and Gallagher & Ney (1976), have shown that the break in the slope between a free-free energy distribution and that of the optically thick Rayleigh-Jeans tail of the pseudophotosphere can be used to estimate the densities in the ejected shells of novae. Unfortunately, we do not have the wavelength coverage in our photometry to accurately estimate where this break occurs. Given the estimate of the density found above ($n_e \geq 10^{10}$ cm^{-3}), the break in the spectrum would occur longward of 3.0 μm, consistent with the shape of the spectral energy distribution observed on March 25.8.

An estimate of the mass of gas ejected in the explosion can be made by assuming that at the time when the ejecta became

TABLE 2

COMPARISON OF DERIVED VALUES OF IMPORTANT PARAMETERS FOR THE OUTBURST OF NOVA HERCULIS 1991

Parameter	H&S[a]	WGJL[b]	CAR[c]	Lloyd[d]	Stfld[e]	Lynch[f]
A_V (mag)	1.4	1.0	0.0	1.5	1.86	1.7
D (kpc)	5.5	2.8	≤ 8.3	10 ± 4	3.4 ± 1.6	3.4
M_V (mag)	−9.7	−9.8	−9.6	−11.1		−9.4
t_3 (days)	5.3	5	6			3.2
L_{max} ($10^5\ L_\odot$)	5.9	1.5	≥ 1	≥ 10		
M_g ($10^{-4}\ M_\odot$)	0.4ϕ[g]	0.9–6.4	0.1	0.1–1		
M_d ($10^{-8}\ M_\odot$)	3.5	32[h]	1.6–2.7			
t_d[i] (days)	8	8	7			

[a] This paper.
[b] Woodward et al. 1991.
[c] Chandrasekhar et al. 1992.
[d] Lloyd et al. 1992.
[e] Starrfield et al. 1992.
[f] Lynch et al. 1992.
[g] ϕ is the filling factor. We believe $\phi \leq 0.04$.
[h] The dust mass quoted by WGJL in their Table 2, $3 \times 10^{-5}\ M_\odot$, should be reduced to $3 \times 10^{-7}\ M_\odot$, as derived in the text of their paper.
[i] Based on $t_0 = 23.0$ 1991 March (WGJL).

optically thin, the opacity of the gaseous shell was dominated by electron (Thomson) scattering. This assumption leads to the relationship: $M_g = \pi R_{\rm shell}^2 \kappa_T$, where κ_T is the Thomson opacity (for hydrogen $\kappa_T = 0.36$ cm^2 g^{-1}), and $R_{\rm shell}$ is the distance of the shell from the central source at the time it becomes optically thin. As discussed, the shell had become optically thin by March 25.8, or $t = t_0 + 2.8$ days. With $v_{\rm exp} = 3500$ km s^{-1}, and $R_{\rm shell} = 8.5 \times 10^{13}$ cm, a shell mass of $M_g = 4.1 \times 10^{-6}$ $M_\odot$ results. A similar value for the shell mass will be derived below.

As noted earlier, the extinction of the spectra increased as the week progressed, while the continua became redder. After attempting, and failing, to model the spectra for March 26.8, 27.8, and 30.8 with normal optically thin gaseous sources for the continua, we added a graybody component to each continuum. That such a continuum source is required to fit the data can best be seen in Figure 5*c*, where the spectrum of a 2000 K blackbody (reddened by $A_V = 1.4$ mag) is presented along with the infrared spectrum for March 27.8. Such a source provides nearly all of the continuum emission in the *K* band for this date, while fitting the lowest continuum points in the *J* and *H* bands. For each of the three days, 26.8–30.8 March, a graybody continuum source with a temperature of 2000 K had to be included to make the model spectra fit the observed spectra. *These spectroscopic observations suggest the presence of dust in the ejecta as early as 2 days after visual maximum*!

That the apparent graybody continuum source is indeed dust is confirmed by the observation that reddening in addition to that from the interstellar component ($A_V = 1.4$ mag) was necessary to obtain properly fitting models of the emission line spectra. On 26.8 March, for example, an additional 1.1 mag of *circumstellar* extinction was used to get a model spectrum whose continuum and H I line ratios matched the observed spectrum. By March 27.8 and 30.8, the circumstellar extinction had increased to $A_V = 2.4$ mag. The appearance of a blackbody-type continuum source with increasing extinction can be best explained as due to the creation of dust amongst the H I emitting gas. It is possible that the grains were pre-existing, a hypothesis we explore below. We will examine this early dust emission phase in considerable detail below.

The final results for both electron temperature and density derived from modeling each of the spectra are listed in Table 3. As the first week following maximum progressed, the electron temperature of the ejecta increased, while the electron density decreased.

4.3. *The Early Formation and Evolution of Dust in the Ejecta*

As noted in § 3.1, N Her underwent a major dust shell formation event between March 30.8 and 31.8. Both the photometry and the spectroscopy for March 31.8 are well fitted by a 2000 K blackbody spectral energy distribution. This is the hottest dust that has ever been observed to form around a nova. In previous dust-producing novae, dust formation has always been observed to occur at a temperature of $T_c \sim 1000$ K (Gehrz 1988, and references therein). A temperature closer to 1000 K would allow the formation of silicates in the ejecta. The high temperature of the N Her dust shell appears to rule out dust composed of normal astrophysical silicates at this early time (see Tielens 1990 for a discussion of the formation temperatures of silicates around late-type stars). This conclusion is also supported by the lack of a silicate feature in the 10 μm photometry presented by WGJL for the early phases of the dust shell evolution. This does not, however, rule out the possibility that silicate grains could have formed at a later time, perhaps using the existing grains as nucleation centers. Such a scenario could explain the 10 μm emission feature observed by Lynch et al. (1992) at $t \simeq +85$ days, which they attribute to silicate emission. The high temperature of the early dust shell does allow the formation of carbon grains. As discussed by CW, carbon grains should begin to condense out of the ejecta once the temperature drops to below 2000 K. We will assume for the remainder of the paper that the grains that formed in the shell of N Her were composed of carbon, and compare their evolution with prediction from the CW model.

TABLE 3

ELECTRON DENSITIES AND TEMPERATURES

Date	T_e (K)	n_e (cm^{-3})
Mar 25.8.....	1000	$\geq 1.0 \times 10^{10}$
Mar 26.8.....	1000	5.0×10^9
Mar 27.8.....	2000	5.0×10^9
Mar 30.8.....	5000	1.0×10^8

By integrating the extracted model continuum attributed to the dust component in the infrared spectra, the total infrared emission arising from just the grains can be estimated at a time when they did not dominate the infrared luminosity of N Her. We have constructed the temporal evolution of the peak of the flux emitted by the dust shell, $[\lambda F_\lambda]_{\rm max}$ versus time since t_0, in Figure 6 for the period March 26.8 to September 26.4. The first three points in Figure 6 are the flux peaks extracted from the spectra, while the remainder result from analysis of our photometry, and some photometry from both Chandrasekhar, Ashok, & Ragland (1992) and WGJL.

The fluxes resulting from the extraction of the dust component of the continuum are model-dependent, and somewhat uncertain. This is especially true for the March 26.8 spectrum, when the dust continuum supplied only 20% of the *K*-band flux. As noted above, however, the dust supplied nearly all of the flux in the *K* band on both March 27.8 and 30.8, leading to much less uncertainty in the derived dust shell luminosity. As can be seen in Figure 6, the luminosity of the dust component more than doubled between March 26.8 and 27.8, then declined between March 27.8 and 30.8. If the dust grains are presumed to have begun to form near March 26.8, and the increase in luminosity between March 26.8 and 27.8 signaled an increase in their size and/or number, it is odd that the dust shell should experience a decline in luminosity from March 27.8 to 30.8. The flux peaks we derive for these two dates are reasonably accurate, and the decline in the dust shell luminosity by a factor of 1.7 is real. If the positions of the dust grains were static (i.e., they were pre-existing), then either the grains decreased in size and/or number during this time, or the luminosity intercepted by them did. If the grains were being created in the ejected gas, then we need to identify a mechanism to explain the drop in emission from these grains.

An insight to what is occurring can be deduced from the fact that the temperature of the grains was 2000 K during the period over which the decline was observed. This indicates that a substantial change in the central source luminosity probably did not occur during this time. Hydrodynamic simulations show that following outburst, a large fraction of the ejected material contracts back onto the white dwarf and enters a phase of hydrostatic equilibrium (Starrfield 1989). The models show that during this phase the remnant maintains a constant

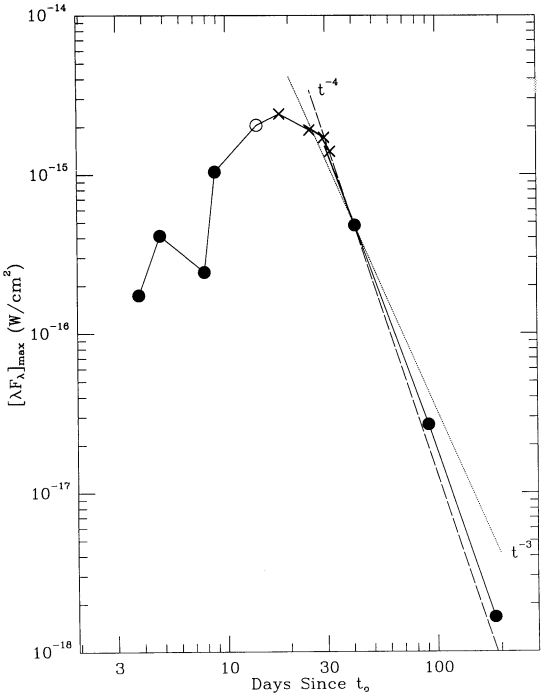

FIG. 6.—Change of the dust shell luminosity, $[\lambda F_\lambda]_{max}$, with time since outburst. The first three points on this plot are the integrated blackbody dust continuum fluxes extracted from the models of the spectra for March 26.8, 27.8, and 30.8, respectively. The data point at 13.97 days, indicated by an open circle, is from Chandrasekhar et al. (1992), while the data at 18, 25, 29, and 31 days after outburst, indicated by crosses, are from WGJL. Shortly after dust shell maximum (day 18), the infrared emission from the dust shell declined as $\lambda F_\lambda \propto t^{-4}$ (*dashed line*, a decline of $\lambda F_\lambda \propto t^{-3}$ is shown as a dotted line).

luminosity. As the pseudo-photosphere recedes, the central source is driven to higher effective temperatures. The result is a central source that emits progressively harder radiation. If the grains are inadequately shielded from the central source, they could be evaporated by the absorption of high-energy photons, a process termed photodesorption. This process destroys grains, diminishing the effective covering area of the dust shell, resulting in less radiation being intercepted and reradiated. Evidence for the hardening of the radiation field is evident from both the rise in the electron temperature (see Table 3), and the increase in the ionization level of the ejecta during this period. While this scenario is plausible, it would seem unlikely that grain destruction by photodesorption could occur without reducing the circumstellar extinction.

One possible model which can explain the unchanging extinction and the eventual formation of the major dust shell is a two component model composed of: (1) large pre-existing grains which are pulverized by the shock during collision with the expanding gas shell, and (2) a significant shell of dust which forms in the gaseous ejecta sometime near March 31.8. An increased number of smaller grains would allow the extinction to remain nearly constant, while the infrared luminosity of the shell would drop due to the fact that smaller grains are less efficient radiators, and that some dust mass is likely to be lost from the system. This scenario seems unlikely for two reasons. The first is that it is more likely that the dust grains would be destroyed during collision with the gas shell, than pulverized by it. Draine (1981) shows that grains are quickly destroyed at shock velocities greater than $v_{exp} \sim 150$ km s^{-1}. The second reason is that it is very difficult to balance the grain properties so that the circumstellar extinction remains constant, while the infrared luminosity declines by a factor of 1.7.

A more reasonable interpretation for the decline in the infrared luminosity of the shell between March 27.8 and 30.8 comes from a calculation of the change in flux intercepted by a dust shell expanding at constant velocity. At any time, the infrared luminosity of a dust shell surrounding a source L_* is $L_{IR} = N_g \pi a^2 Q_a L_* / 4\pi R_{shell}^2$ (Gehrz et al. 1980b), where N_g is the number of dust grains, a is the grain radius, Q_a is the Planck mean absorption cross section, and R_{shell} the shell radius. If we assume a constant luminosity central source, and that a, N_g and Q_a do not change, then the ratio of the shell luminosities at any two times is: $L_{IR_1}/L_{IR_2} = R_{shell_2}^2/R_{shell_1}^2$. The observed value of this ratio was 0.6, while the calculated ratio is 0.4; reasonable agreement, given the uncertainty in determining the shell luminosities. This simple calculation implies, however, that the grains must not have grown very much during this interval.

Between March 30.8 and 31.8, the major dust shell condensed. A model which explains the sudden onset of dust formation must consider the radiation field present in the circumstellar environment. WGJL note that the dynamical dust-condensation timescale (t_c) is given by $t_c = R_c v_{exp}^{-1} = v^{-1} (L_*/16\pi\sigma T_c^4)^{1/2}$, where R_c is the condensation radius, v_{exp} is the expansion velocity in km s^{-1}, L_* is the luminosity of the central source in $L_\odot$, and T_c is the dust condensation temperature in K. Using $v_{exp} = 3500$ km s^{-1}, $L_* = 5.9 \times 10^5\ L_\odot$, and $T_c = 2000$ K, the calculated dust condensation timescale for N Her was $t_c = 7.5$ days. The major dust formation epoch began between 7.8 and 8.8 days after outburst (see Fig. 3*b*). The agreement between the predicted time and the observed time of dust shell formation shows that at the onset of the rapid grain formation phase, the dust was in radiational equilibrium with a central source whose luminosity had not changed since visual maximum. Rapid dust formation proceeded once the ejected shell had reached a distance such that the radiation equilibrium temperature with the central source had dropped below the dust condensation temperature.

On day 8.8, the optical depth of the dust shell was $\tau \simeq 0.02$. A similar calculation for the WGJL photometry on day 18 yields $\tau \simeq 0.05$. As CW point out, the total number of grains formed in a nova shell should change very little once the formation process has begun. The increase in optical depth observed was probably due to the increase in size of the individual grains. How much the grains grew during this interval can be appraised using the knowledge that at any given time the infrared luminosity of a dust shell is $L_{IR} = N_g 4\pi a^3 \sigma T_g^4 (Q_e/a)$ (Gehrz et al. 1980a). In this equation N_g is the number of grains, a is the grain radius, T_g is the temperature of the grains, and Q_e is the Planck-mean emission cross section for a carbon grain of radius a. If we assume that during the grain-growth interval N_g remains constant, and that $Q_e/a = 0.01 T_g^2$ (from Gilman 1974, applicable for carbon grains with $a \leq 1$ μm), then the ratio of the infrared luminosities at different times leads to a relation for the ratio of the grain radii: $a_2/a_1 = (L_{IR_2}/L_{IR_1})^{1/3} (T_{g_1}/T_{g_2})^2$. For the parameters noted above, we obtain $a_2/a_1 = 4.0$. We find that the grain radii grew by about a factor of 4 between days 8 and 25. This is consistent with the CW model, which predicts rapid grain growth shortly after formation begins.

Further insight into the structure of the gaseous shell and evolution of the dust shell can be obtained through further comparison of the CW model with the infrared observations. This model predicts that the time of dust-shell maximum is

$t_{max} = Ct_c$, where t_c is the time at which grain growth starts, and the constant C lies in the range 2.3 to 2.5. For $t_c = 8$ days, the time of dust shell maximum is then $t_{max} = 18.6$ to 20 days; in excellent agreement with the observed time of dust shell maximum of 18 to 20 days after outburst (see Fig. 6). The CW model also predicts that the infrared luminosity of a dust shell expanding at constant velocity declines as $L_{IR} \propto t^{-2}$. WGJL have fit the early decline of the infrared luminosity with such a power law (their Fig. 3*b*), and with their limited coverage such a fit it not unrealistic. However, from the longer time coverage presented in Figure 6, we find that the WGJL data actually defines a brief plateau in the infrared luminosity near dust-shell maximum, tending toward a steeper (t^{-4}) decline thereafter. WGJL do show (their Fig. 3*a*) that the early decline of the temperature of the dust shell of N Her, $T_d \propto t^{-1/2}$, was consistent with a model where optically thick clumps of fixed size moved away at constant velocity from a constant luminosity central source. If the dust resides in the gas clumps, then we can use this model to determine the distribution and quantity of matter in the ejected shell. This is done in the following section.

4.4. *Estimating the Filling Factor and Mass of the Gas and Dust in the Ejecta of N Her*

Earlier we estimated an ejected gas mass of $4.1 \times 10^{-6}\ M_\odot$ from arguments about when the gaseous shell became optically thin. Accurate estimates of the ejected mass require knowledge of how the gas is distributed. As has been shown elsewhere (e.g., Mustel & Boyarchuk 1972; Seaquist et al. 1989), the ejected shells of novae are very clumpy. Estimates of the measure of this clumpiness in novae ejecta, the filling factor (ϕ), range from as large as $\phi = 0.25$ (for DQ Her; Martin 1989), to intermediate values, $\phi = 0.1$ (for HR Del; Peimbert & Sarmiento 1984), to the very low value of $\phi = 1.7 \times 10^{-5}$ (for V1370 Aql; Snijders et al. 1984). We can derive an upper limit to the filling factor by assuming spherical, optically thick clumps containing all of the gas and dust, moving outward at the expansion velocity. The projected area subtended by the clumps is equal to the fraction (τ) of the spherical shell intercepted by the clumps: $N_{cl}\pi R_{cl}^2 = \tau 4\pi v_{exp}^2 t^2$, or $R_{cl} = 2v_{exp}t(\tau/N_{cl})^{1/2}$. The filling factor is simply: $\phi = N_{cl}V_{cl}/V_{shell} = 8N_{cl}^{-1/2}\tau^{3/2}$. At maximum, the dust shell intercepted 5% of the luminosity of the central engine (i.e., $\tau = 0.05$), thus $\phi = 0.089N_{cl}^{-1/2}$. This equation shows that the filling factor must have been less than 0.1. Optical spectra revealed that the Hα line had at least five components (Feast 1991), and if these represent individual clumps, then the filling factor is not larger than $\phi = 0.04$. Thus, the filling factor for the ejecta of N Her appears to have been low.

With an estimate of the filling factor we can calculate an upper limit to the mass of the ejected gaseous shell using: $M_g = n_e \phi V_{shell}\ m_H$, where n_e is the electron density, ϕ is the filling factor, V_{shell} is the volume of the ejected shell ($4\pi v_{exp}^3 t^3/3$), and m_H is the mass of the hydrogen atom. Using $\phi = 0.04$, an expansion velocity of 3500 km s^{-1}, and the electron densities listed in Table 3, the average value for the ejected gas mass is $M_g = 1.1 \times 10^{-6}\ M_\odot$. This value is similar to that which we determined earlier using the electron scattering argument, but significantly lower than the other published values (see Table 2). We believe that due to the clumpy nature of the ejecta, it is inappropriate to assume thin spherical shells when calculating the ejected mass, and in reality, our result represents an *upper limit* to the gas mass implied using the clump model. Under this model, higher masses for the ejecta result only by assuming higher expansion velocities, an earlier outburst date, or higher density ejecta. We cannot see how any of these parameters can be altered too far from the values which we have used in the above derivation.

An estimate of the dust mass, M_d, can be found using the relationship $M_d = (L_{IR}\rho_g)/[3\sigma T_d^4(Q_e/a)]$, where L_{IR} is the luminosity of the dust shell, and ρ_g is the density of carbon grains (2.25 g cm^{-3}, Gehrz et al. 1980b). Using $Q_e = 0.01aT_d^2$ (Gilman 1974) and $T_d = 1100$ K, we find that $M_d = 1.1 \times 10^{-8}\ M_\odot$ at dust shell maximum. This results in a gas-to-dust ratio of $M_g/M_d \simeq 100$, similar to the interstellar value (Spitzer 1978, p. 162).

4.5. *The Temporal Evolution of the Central Source and the Dust Shell Luminosities*

We can make use of the temperature of the dust shell at various epochs to determine the temporal evolution of the central source luminosity. As we have shown above, on day 8.8, the time of dust shell formation, the central source had a luminosity of $5.9 \times 10^5\ L_\odot$, the same luminosity as we derived for visual maximum using the t_3 relationship. By day 13.97 (April 5.97), the date of the first photometry by Chandrasekhar et al. (1992), a similar calculation gives a central source luminosity of $1.6 \times 10^5\ L_\odot$ (using $T_d = 1500$ K). For the WGJL data on days 18 and 25, we derive a central source luminosity of $1.5 \times 10^5\ L_\odot$, in agreement with their determination.

N Her appears to have maintained a very high luminosity for about the first week following visual maximum, and then declined by a factor of 3.7 to a lower plateau-luminosity which it maintained for (at least) the next 2 weeks. At visual maximum, the luminosity of the central engine was a factor of $\sim$13 above the Eddington luminosity for a 1.4 $M_\odot$ white dwarf, dropping to a factor of $\sim$3 above this luminosity at dust shell maximum. The Eddington limit is composition dependent, and if the accreted envelope contained a significant percentage of helium and other heavier elements, the super-Eddington luminosities, derived above for hydrogen, would be substantially reduced (by a factor of $\simeq$2 in the pure helium case). The scenario where N Her was super-Eddington for a brief period, and then dropped back to a more stable luminosity closer to the Eddington luminosity, is consistent with hydrostatic simulations of novae outbursts (Starrfield 1989).

Starting about 25 days after outburst, both the infrared luminosity and temperature of the dust shell began to deviate from the evolution predicted by the clump model detailed above. At this time the infrared luminosity began a steep decline, $L_{IR} \propto t^{-4}$, while the temperature of the shell began to decline more slowly than the $T_d \propto t^{-1/2}$ relationship adhered to earlier. As discussed above the infrared luminosity of a dust shell can be found from the relationship: $L_{IR} = N_g \pi a^2 Q_a L_* / 4\pi R_{shell}^2$. Substituting vt for R_{shell}, the infrared luminosity is $L_{IR} \propto N_g a^2 Q_a L_* t^{-2}$. If the infrared luminosity is declining as $L_{IR} \propto t^{-4}$, then either the central source luminosity is declining as t^{-2}, or the grains are changing their size (which affects a, N_g, and Q_a), or a combination of these processes is occurring.

A key to interpreting the decline in shell luminosity is found in the change in the rate of cooling exhibited by the dust grains. Gehrz et al. (1980a) have shown that the temperature of a small graphite grain flowing outward at constant velocity from a constant luminosity central source should decline as $T_g \propto$

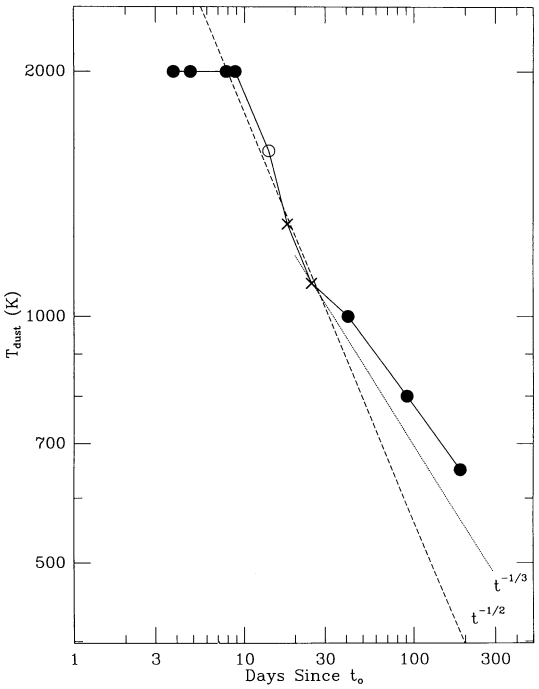

FIG. 7.—Change in the dust shell temperature as a function of time. The dust condensed at a temperature of 2000 K. At first, the temperature of the dust shell declines as $t^{-1/2}$ (*dashed line*). Shortly after dust shell maximum (day 25) the temperature of the shell departs from the $t^{-1/2}$ relation. Gehrz et al. (1980a) have shown that the temperature of a graphite grain flowing outward at constant velocity from a constant luminosity central source should decline as $T_g \propto t^{-1/3}$ (*dotted line*). The data point for day 13.97 (*open circle*) is from Chandrasekhar et al. (1992), while the points for days 18 and 25 (*crosses*) are from WGJL.

$t^{-1/3}$. As is apparent from Figure 7, the temperature decline rate was somewhat slower than this. A handful of novae have exhibited similar behavior. The dust shell of LW Serpentis actually showed a temperature increase (Gehrz et al. 1980a), while the shell of NQ Vul underwent an "isothermal" phase (Ney & Hatfield 1978). In both cases, a reduction in the size of the grains has been invoked to explain this behavior. It seems plausible to assume that a similar process was occurring in the dust shell of N Her.

A number of methods have been applied to explain how dust grains could be destroyed/sputtered in the hostile nova environment. Mitchell & Evans (1984), and Mitchell, Evans, & Albinson (1986) investigated various chemical sputtering scenarios. In both cases, the dust grain destruction scenario involved the existence of an optically thick dust shell—certainly not applicable to the case of N Her. Recently, Johnson et al. (1993) have shown how effective the process of photodesorption can be in limiting the initial grain growth. We suggest that dust destruction through photodesorption is the most reasonable scenario to explain the slow temperature decline rate observed for N Her.

5. DISCUSSION

The discussion detailed above leads to the following summary of the temporal evolution of the outburst of N Her. The initial outburst of N Her occurred on or near 1991 March 23.0 (t_0). N Her reached a visual maximum of $m_v = 5.4$ on March 24.8. Within one day of visual maximum, the gaseous ejecta had become optically thin well into the near-infrared. The gaseous ejecta were very dense ($n_e \geq 10^{10}$ cm^{-3}), and very cool ($T_e = 1000$ K) at this time. Within 2 days of visual maximum, a limited quantity of dust began to form in the ejecta, as evidenced by the change in the continuum and the increased extinction in the hydrogen lines. By March 27.8, hot, 2000 K dust supplied nearly all of the K-band continuum. Throughout this first week, a pronounced J-band excess (at $\lambda > 1.17$ μm) was present, which slowly declined in intensity as the excitation level of the ejecta increased. Between March 30.8 and 31.8 a major dust-shell formation event occurred. The temperature of this dust shell, $T_d = 2000$ K, is the hottest ever observed to have formed in a nova. The dust shell reached its maximum optical depth between 18 and 20 days after t_0. The early evolution of the dust shell is well modeled by a scenario where optically thick clumps of carbon dust move outward with constant velocity. At late times, the luminosity and temperature evolution of the dust shell indicate a period of dust destruction likely occurred. Eventually, the luminosity of the dust shell faded to the point where from sources other than the dust were dominating the J- and H-band fluxes.

We have seen in the above that N Her was an unusual nova in several respects. The infrared spectrophotometric observations have shown that a limited amount of dust was present in the ejecta within two days of visual maximum. We suggest that this dust was created within the gaseous ejecta. The creation of dust so close to visual maximum would be without observational procedence. That the dust which formed during this period maintained a temperature of 2000 K argues strongly for this being the formation temperature of the dust grains, confirming the CW scenario for carbon grains. We have argued that the formation of dust in the ejecta caused the infrared flux to decline more slowly ($F_\lambda \propto t^{-1}$) than it would have if the only source of radiation were free-free emission from the ejected gas. It is difficult to extract this type of information without infrared spectrophotometry. Other novae, such as PW Vul (Gehrz et al. 1988), which have exhibited similar slow declines in their infrared fluxes, might be cases where a similar period of limited grain growth occurred.

That the ejecta of N Her were optically thin within one day of visual maximum is surprising, and in stark contrast to V1500 Cyg, another very fast nova. V1500 Cyg maintained an optically thick pseudophotosphere for two days following visual maximum (Gallagher & Ney 1976; Ennis et al. 1977). K-band spectra of V1500 Cyg at this time revealed H I Brγ absorption (Ennis et al. 1977). V1500 Cyg does not appear to have formed dust. The outburst of V1500 Cyg differs from N Her in that the expansion velocity of its ejecta was lower, its luminosity was higher, and it apparently ejected a significantly more massive gaseous shell. The contrast between two of the fastest and most luminous novae ever observed is dramatic.

While the density of the ejecta found for N Her on March 25.8 is not too surprising (similar to V1500 Cyg shortly after visual maximum, Ennis et al. 1977), the low electron temperature certainly is. Even a small change in T_e to 3000 K causes the model Brackett continuum to deviate substantially from the observed spectrum. It is surprising that the gaseous ejecta, expected to be $\sim$6000 K at visual maximum, could have cooled to 1000 K in only 24 hours. Free-free emission, however, is dependent on the product of the electron and ion densities, and with $n_e \simeq 10^{11}$ cm^{-3}, a significant amount of cooling is possible from this process alone. If we take the effective temperature of N Her at visual maximum to be 6000 K, and the masses of the ejected gaseous shell to be 1.1×10^{-6}

$M_\odot$, the thermal energy content of the gaseous shell would have been $E_{th} = (3/2)NkT_{gas} = 1.6 \times 10^{39}$ ergs. One day later, when $T_{gas} = 1000$ K, the thermal energy of the shell was $E_{th} = 2.7 \times 10^{38}$ ergs. The thermal energy radiated in 24 hours was 1.3×10^{39} ergs, or a luminosity of 1.5×10^{34} ergs s^{-1}. We calculate that the free-free luminosity of the gaseous ejecta arranged in clumps ($\phi = 0.04$), with $n_e = n_p = 10^{11}$ cm^{-3}, was $L_{ff} = 3.6 \times 10^{38}$ ergs s^{-1} (we have set the free-free Gaunt factor to 1.0). The luminosity from the central source intercepted by the clumps on March 25.8 ($L_* = 5.9 \times 10^5\ L_\odot$, and assuming $\tau = 0.05$) was 1.2×10^{38} ergs s^{-1}. The gas clumps are easily able to radiate away both their thermal energy and the intercepted luminosity in the 24 hours following visual maximum through free-free radiation.

We close by noting that further modeling is necessary to understand the origin of a number of unidentified features in the infrared spectra discussed above. The conjecture that [Ne I] or C_2 emission could explain the observed features needs to be explored. Neon should be abundant in the ejecta of an ONeMg nova, while Johnson et al. (1993) show that C_2 is an important building-block in the grain growth process. Modeling the infrared nebular emission spectra of these two species should be undertaken. Optical spectra obtained during the first week following visual maximum should be examined to determine if C_2 emission features were present.

The authors would like to thank J. Johnson and P. te Lintel Hekkert for allowing us to obtain observations during time scheduled to them, P. McGregor who assisted us in bringing CIGS back on-line, and R. McNaught for alerting us early on to the outburst of N Her. We would also like to thank R. Gehrz and S. Shore for helpful discussions, and J. Spyromilio for assistance with the modeling program.

REFERENCES

Alcock, G. 1991, IAU Circ. No. 5222
Bath, G. T. 1978, MNRAS, 182, 35
Boyarchuk, A. A., & Gershberg, R. E. 1977, Soviet Astron., 21, 275
Brault, J. W., et al. 1982, A&A, 108, 201
Buczynski, D. 1991, IAU Circ. No. 5224
Chandrasekhar, T., Ashok, N. M., & Ragland, S. 1992, MNRAS, 255, 412
Clayton, D. D., & Wickramasinghe, N. C. 1976, Ap&SS, 42, 463 (CW)
Cohen, J. G. 1988, in Instrumentation for Ground-Based Optical Astronomy, ed. L. B. Robinson (New York: Springer), 448
Della Valle, M., & Turrato, M. 1991, IAU Circ. No. 5223
Dopita, M., Ryder, S., & Vassiliadis, E. 1991, IAU Circ. No. 5262
Draine, B. T. 1981, ApJ, 245, 880
Draine, B. T., & Salpeter, E. E. 1979, ApJ, 231, 438
Ennis, D., Becklin, E. E., Beckwith, S., Elias, J., Gatley, I., Matthews, K., Neugebauer, G., & Willner, S. P. 1977, ApJ, 214, 478
Evans, A., Callus, C. M., Whitelock, P. A., & Laney, D. 1990, MNRAS, 246, 527
Feast, M. W. 1991, IAU Circ. No. 5233
Gallagher, J. S., & Anderson, C. M. 1976, ApJ, 203, 625
Gallagher, J. S., & Ney, E. P. 1976, ApJ, 204, L35
Gehrz, R. D., Grasdalen, G. L., Hackwell, J. A., & Ney, E. P. 1980a, ApJ, 237, 855
Gehrz, R. D. 1988, ARA&A, 26, 377
Gehrz, R. D., Hackwell, J. A., Grasdalen, G. L., Ney, E. P., Neugebauer, G., & Sellgren, K. 1980b, ApJ, 239, 570
Gehrz, R. D., Harrison, T. E., Ney, E. P., Matthews, K., Neugebauer, G., Elias, J., Grasdalen, G. L., & Hackwell, J. A. 1988, ApJ, 329, 894
Gehrz, R. D., Jones, T. J., Woodward, C. E., Greenhouse, M. A., Wagner, R. M., Harrison, T. E. Hayward, T. L., & Benson, J. 1992, ApJ, 400, 671
Gehrz, R. D., Ney, E. P., Grasdalen, G. L., Hackwell, J. A., & Thronson, H. A. 1984, ApJ, 281, 303
Gilman, R. C. 1974, ApJS, 28, 397
Goebel, J. H., et al. 1980, ApJ, 235, 104
Greenhouse, M. A., Grasdalen, G. L., Woodward, C. E., Benson, J., Gehrz, R. D., Rosenthal, E., & Skrutski, M. F. 1990, ApJ, 352, 307
Harrison, T. E., Johnson, J. J., & Spyromilio, J. S. 1993, AJ, 105, 320
Harrison, T. E., & Stringfellow, G. S. 1994, in preparation
Hummer, D. G., & Storey, P. J. 1987, MNRAS, 224, 801 (HS)
Izumo, A., & Oshima, O. 1991, IAU Circ. No. 5234
Johnson, J. R., Fink, U., & Larson, H. P. 1983, ApJ, 270, 769
Johnson, D. J., Friedlander, M. W., & Katz, J. I. 1993, ApJ, 407, 714
Jones, T. J., et al. 1982, PASP, 94, 207
Lance, C. M., McCall, M. L., & Uomoto, A. K. 1988, ApJS, 66, 151
Lloyd, H. M., O'Brien, T. J., Bode, M. F., Predehl, P., Schmitt, J. H. M. M., Trumper, J., Watson, M. G., & Pounds, K. A. 1992, Nature, 356, 222
Lynch, D. K., Hackwell, J. A., & Russel, R. W. 1992, ApJ, 398, 632
Martin, P. G. 1989, in Classical Novae, ed. M. F. Bode & A. Evans (New York: Wiley), 93
Matheson, T., Fillippenko, A. V., & Ho, L. C. 1993, ApJ, 418, L29
McGregor, P. J. 1994, PASP, 106, 508
McLaughlin, D. B. 1960, in Stars and Stellar Systems VI, Stellar Atmospheres, ed. J. L. Greenstein (Chicago: Univ. Chicago Press), 585
McNaught, R. H. 1991, IAU Circ. No. 5223
Miroshnichenko, A. S. 1988, Soviet Astron., 32, 298
Mitchell, R. M., & Evans, A. 1984, MNRAS, 209, 945
Mitchell, R. M., Evans, A., & Albinson, J. S. 1986, MNRAS, 221, 1057 (MEA)
Mustel, E. R., & Boyarchuk, A. A. 1972, ApSS, 6, 183
Ney, E. P., & Hatfield, B. F. 1978, ApJ, 219, L11
Peimbert, M., & Sarmiento, A. 1984, Astron. Express, 1, 3
Seaquist, E. R., Bode, M. F., Frail, D. A., Roberts, J. A., Evans, A., & Albinson, J. S. 1989, AJ, 344, 805
Snijders, M. A. J., Batt, T. J., Seaton, M. J., Blades, J. C., & Morton, D. C. 1984, MNRAS, 211, 7P
Sonneborn, G., Shore, S., & Starrfield, S. 1991, IAU Circ. No. 5226
Sowell, J. R. 1987, ApJS, 64, 241
Sparks, W. M., Starrfield, S. G., & Truran, J. W. 1976, ApJ, 208, 819
Spitzer, L. 1978, Physical Processes in the Interstellar Medium (New York: Wiley)
Starrfield, S. G., Sparks, W. M., & Truran, J. W. 1986, ApJ, 303, L5
Starrfield, S. G. 1989, in Classical Novae, ed. M. F. Bode & A. Evans (New York: Wiley), 39
Starrfield, S., Shore, S. N., Sparks, W. M., Sonneborn, G., Truran, J. W., & Politiano, M. 1992, ApJ, 391, L71
Sugano, M. 1991, IAU Circ. No. 5222
Tielens, A. G. G. M. 1990, in From Miras to Planetary Nebulae: Which Path for Stellar Evolution, ed. M. O. Mennessier & A. Omont (Gif-sur-Yvette: Editions Frontières), 186
van den Bergh, S., & Younger, P. F. 1987, AAS, 70, 125
Vogt, N. 1990, ApJ, 356, 609
Woodward, C. E., Gehrz, R. D., Jones, T. J., & Lawrence, G. F. 1992, ApJ, 384, L41 (WGJL)
Yamamoto, M. 1991, IAU Circ. No. 5226